DOI: 10.1002/ejoc.201300339

Functionalized Gold Nanoparticles as an Approach to the Direct Colorimetric Detection of DCNP Nerve Agent Simulant

Almudena Martí,[a,b] Ana M. Costero,[a,b] Pablo Gaviña,*[a,b] Salvador Gil,[a,b] Margarita Parra,*[a,b] Mauro Brotons-Gisbert,[c] and Juan Francisco Sánchez-Royo[c]

Keywords: Gold / Nanoparticles / Sensors / Nerve agents / Colorimetry

New functionalized gold nanoparticles have been synthesized and their ability to act as colorimetric molecular probes for the naked-eye detection of nerve agent simulant DCNP has been studied. The detection process is based on the compensation of charges at the surfaces of the functionalized AuNPs, which triggers their aggregation with the resulting change in the color of the solution.

Introduction

The use of chemical warfare (CW) agents in terrorist attacks has proven the need for the development of reliable and accurate methods for detecting these lethal compounds.[1] Among CW weapons, nerve agents are especially dangerous and the United Nations classifies them as weapons of mass destruction. Nerve agents are capable of interfering with the action of the nervous system. Their primary mode of action is the inhibition of acetylcholinesterase, resulting in an accumulation of acetylcholine in the synaptic junctions, which hinders the relaxing of muscles.[2]

Analytical methods based on enzymatic assays and physical measurements have generally been used to detect these agents.[3] However, these protocols usually have limitations, such as low selectivity, poor portability and a certain level of complexity. In recent years several chromo- and fluorogenic sensors and probes for nerve agents have been described.[4] Colorimetric detection is particularly appealing because it uses low-cost, widely available instruments and allows assays to be detected by the naked eye. Our research group has developed a new family of reagents for the chromogenic detection of the nerve agent simulants DFP, DCP and DCNP (Figure 1) based on the use of 2-[2-(dimethylamino)phenyl]ethanol reactive groups that are part of the conjugated π system of donor–acceptor dyes.[5] The nucleophilic hydroxy group of this moiety is easily phosphorylated by nerve agent simulants to give the intermediate **II** (Scheme 1, a), which undergoes rapid intramolecular *N*-alkylation to afford the quaternary ammonium salt **III**. The change in the electronic distribution promoted by these processes allows the colorimetric detection of DCP, DFP and DCNP, whereas the reagents remain silent in the presence of other organophosphorus derivatives. On the other hand, the nucleophilic reactivity of the pyridine moiety of a push–pull azo dye towards nerve gases has allowed us to develop off–on colorimetric sensors (Scheme 1, b).[6]

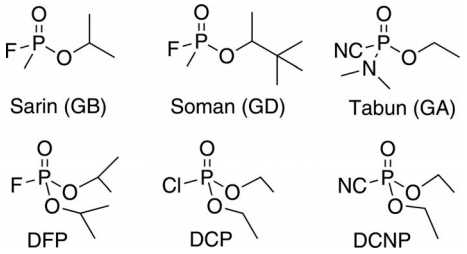

Figure 1. Chemical structures of different organophosphorus nerve reagents and their simulants.

In both cases, the reaction between the probe and the simulant generates a positive charge on the molecule. Based on this fact, we focused on the study of the behaviour of gold nanoparticles (AuNPs) functionalized with this type of moiety towards nerve agents. The functionalization of AuNPs has attracted research interest, especially in receptor-based sensor applications.[7] Gold nanoparticles have unique optoelectronic properties that can easily be tuned by changing their size, shape or chemical environment.[7–9] Colorimetric assays based on gold nanoparticles have recently become useful for many types of analytes without the need for advanced instrumentation because the molecular

[a] Centro de Reconocimiento Molecular y Desarrollo Tecnológico (IDM), Unidad Mixta Universidad de Valencia-Universidad Politécnica de Valencia,
Valencia, Spain
Fax: +34-963543151
E-mail: pablo.gavina@uv.es
margarita.parra@uv.es
Homepage: http://idm.webs.upv.es
[b] Departamento de Química Orgánica, Universidad de Valencia, c/ Dr. Moliner 50, 46100 Burjassot, Valencia, Spain
Homepage: http://www.uv.es/
[c] Instituto de Ciencia de los Materiales, Universidad de Valencia, c/ Dr. Moliner 50, 46100 Burjassot, Valencia, Spain
Homepage: http://www.uv.es

Supporting information for this article is available on the WWW under http://dx.doi.org/10.1002/ejoc.201300339.

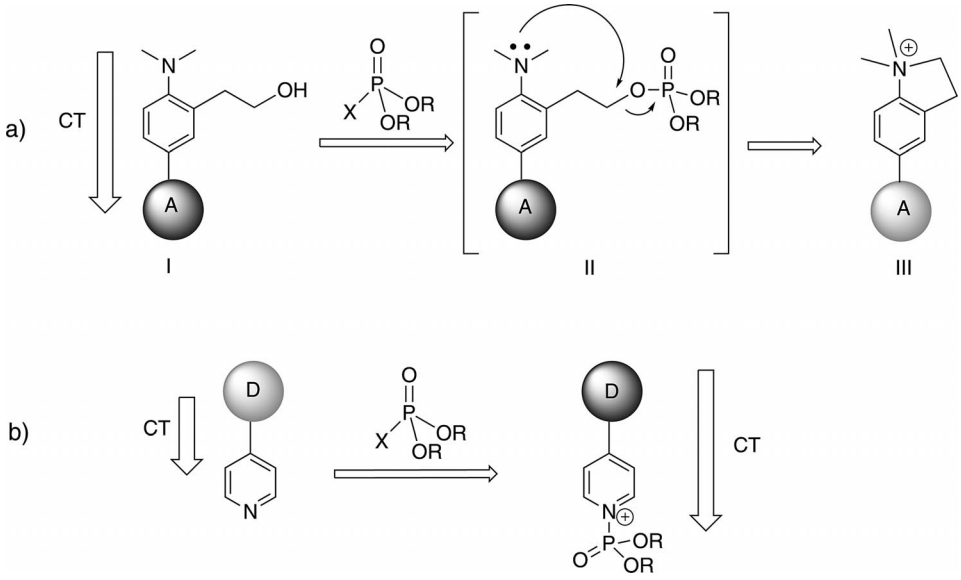

Scheme 1. Colorimetric sensing paradigm developed by our group.

recognition events can be transformed into color changes.[10] The selective and sensitive strategy for sensing is based on the color change that arises from the interparticle plasmon coupling that occurs during aggregation of AuNPs or the dispersion of AuNP aggregates. The red color of dispersed nanoparticles turns to dark blue upon aggregation, and this color change can be observed by the naked eye even at low concentrations.[11] Thus, the generation of positive charges on the surfaces of dispersed functionalized anionic AuNPs as a result of their reaction with nerve agents will induce their aggregation with the concomitant color change.

Recently, the detection of highly toxic organophosphate pesticides by using thioctic acid capped AuNPs as colorimetric probes in an indirect strategy with very low detection limits has been described.[7c,12,13] In that research sensors were developed for the detection of thiocholine obtained by catalytic hydrolysis of acetylthiocholine by acetylcholinesterase. The ligand-exchange reaction between cationic thiocholine and the negatively charged thioctic carboxylate induces the aggregation of Au nanoparticles. The irreversible inhibition of acetylcholinesterase by the organophosphorus pesticides prevents aggregation and the red color of the Au nanoparticles remains.

Following a completely different approach, we report herein the results obtained in the direct detection of DCNP (as simulant of tabun) by using thioctic acid capped AuNPs functionalized with pyridines or 2-[2-(dimethylamino)phenyl]ethanol derivatives.

Results and Discussion

The sensing paradigm of the detection process, which is presented in Scheme 2, involves the generation of positive charges on the surfaces of the gold nanoparticles through the reactions of the terminal nucleophilic ligands with molecules of the nerve agent simulant. These positive charges partially neutralize the original negative charges of the nanoparticles, inducing their aggregation and thus a change in their surface plasmon resonance absorption and consequently a change in their color.

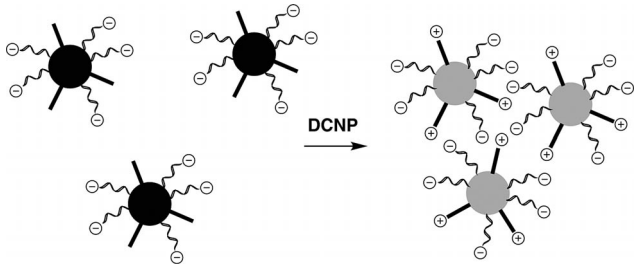

Scheme 2. Paradigm of the sensing mechanism. Reaction of the terminal ligands with the simulant produces positive charges that can compensate the negative charges of the AuNPs and induce aggregation processes.

Synthesis of the Ligands

AuNPs have affinity for both reduced (thiols) and oxidized (disulfide) sulfur groups through Au–S bonds, and thus both groups can be used as anchors for the functionalization of nanoparticles. The different ligands used in this study are presented in Figure 2.

Ligands **1** and **2** are commercially available, whereas **3** and **4** were obtained by the esterification of the corresponding alcohol or disulfide derivatives with thioctic acid (TA) under Steghich[14] or Mitsunobu[15] conditions. Ligands **5**–**7** were synthesized by an azo-coupling reaction between pyridine-4-diazonium (obtained from 4-aminopyridine by diazotization) and phenol, *N*-phenyl-*N*-methyl-2-amino-

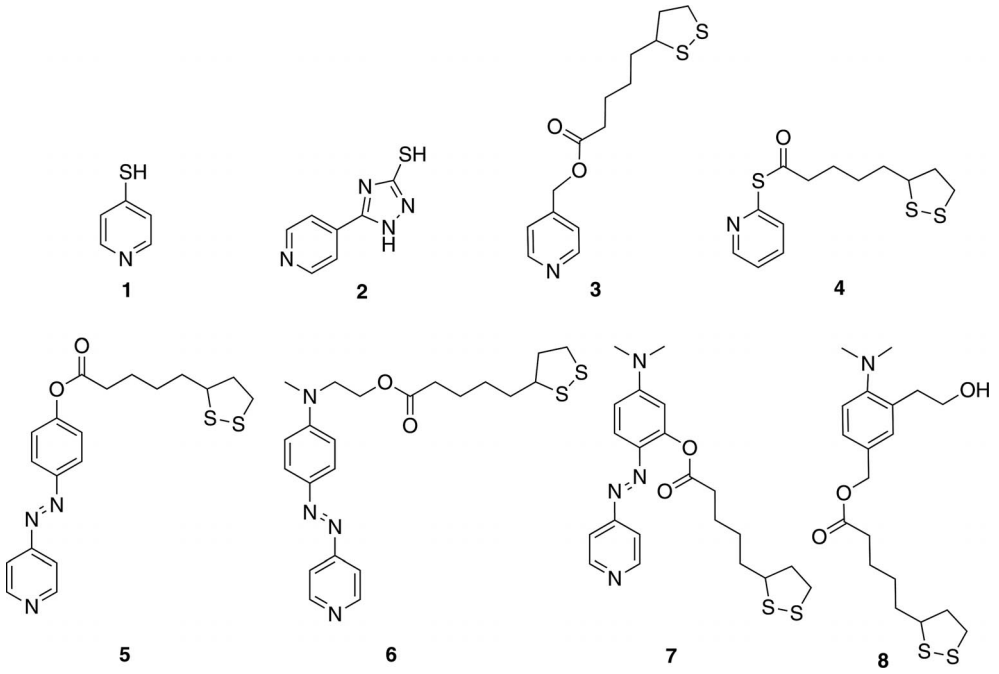

Figure 2. Ligands **1**–**8** synthesized for the functionalization of AuNPs.

ethanol or 3-(dimethylamino)phenol, respectively, followed by esterification with TA. Ligand **8** required a seven-step synthesis and is depicted in Scheme 3. Thus, 2-(2-nitrophenyl)ethanol (**9**) was reduced in the presence of formaldehyde to the corresponding dimethylamino derivative **10**. This amino compound was transformed into the 4-bromo derivative **11** by reaction with *N*-bromosuccinimide (NBS). Protection of the hydroxy group as a silyl ether yielded **12**, which was lithiated with BuLi and then transformed into the formyl derivative **13** by reaction with DMF. Compound **13** was subsequently reduced to the corresponding benzylic alcohol **14**. After esterification with thioctic acid and deprotection of the silyl-protected hydroxy moiety with *tert*-butylammonium fluoride (TBAF), ligand **8** was obtained in a 20% overall yield. The chemical structures and purity of ligands **1**–**8** were confirmed by spectroscopic techniques.

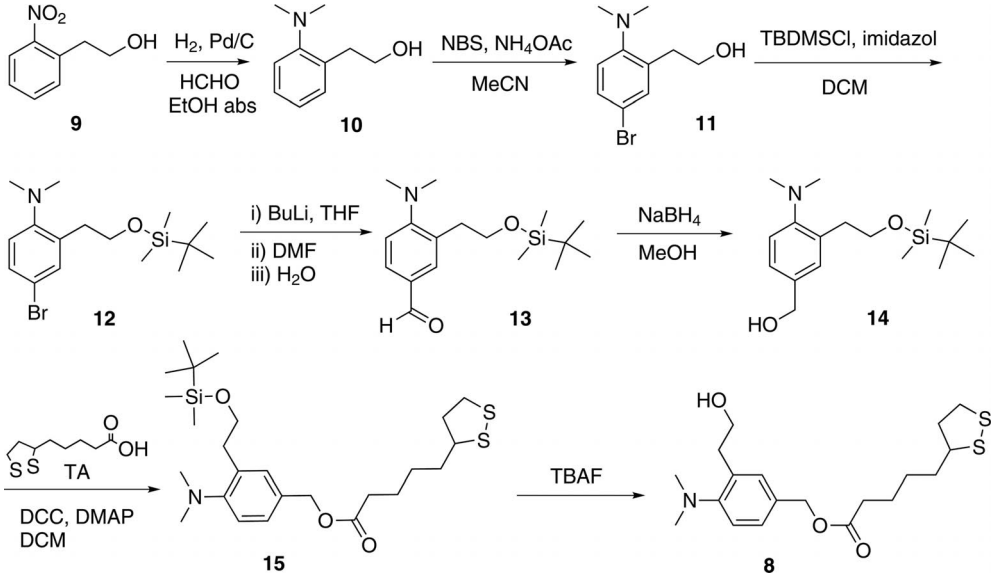

Scheme 3. Synthesis of ligand **8**.

Synthesis of the Functionalized Gold Nanoparticles

AuNPs can be synthesized by different procedures,[16–18] the size, stability and optical properties of the resulting nanoparticles being strongly dependent upon the method used. The functionalized gold nanoparticles AuNP**1**-AuNP**8** were synthesized by a two-step procedure. First, citrate-stabilized nanoparticles were prepared by reducing tetrachloroauric acid with trisodium citrate in boiling water.[8,19] In this step we found that both the relative concentration of the reagents and thorough cleaning of the glassware with aqua regia were crucial to avoid either nucleation during the synthesis or aggregation of the gold colloid solutions. Monodisperse citrate-stabilized nanoparticles were thus obtained with an average size of 13 nm, as determined by TEM. The surface plasmon peak appears at 526 nm, in perfect agreement with the experimental data for particle sizes smaller than 25 nm.[8] The molar extinction coefficient was estimated to be $\varepsilon = 2.47 \times 10^8$ M^{-1} cm^{-1} (obtained from the plot of ε vs. nanoparticle size reported by Huo and co-workers[20]). The initial concentration of the citrate-capped AuNPs was calculated from the Beer–Lambert law to be 5.3×10^{-9} M.

In the second step, in a ligand-exchange reaction, the citrate was displaced from the surface of the nanoparticles by a mixture of thioctic acid and the different ligands **1**–**8**. In each case it was necessary to optimize the ligand/TA molar ratio (from 1:1 to 1:4) to improve the stabilization of the nanoparticles as well as the response with respect to the analyte.

As an alternative, a three-step protocol was tested for the functionalization of AuNPs in which the citrate was first displaced by TA and the resulting TA-capped AuNPs were stirred in the presence of ligands for a second ligand-exchange reaction. However, the degree of functionalization was much lower by this method, as evidenced by a weaker response towards the war agent simulant.

In this study, the nanoparticles were centrifuged and redissolved in a buffered aqueous solution (MOPS) at pH 7. In this medium, no obvious change either in color nor in the characteristic peak at 526 nm was observed.

The resulting functionalized gold nanoparticles were characterized by UV/Vis and zeta-potential measurements, and the results are summarized in Table 1. In some cases the AuNPs were also characterized by TEM or XPS.

Table 1. Characterization of the gold nanoparticles.[a]

AuNP	Optimized TA:L molar ratio	SPR peak λ_{max} [nm]	c [M]	ζ-potential [mV][b]
AuNP**2**	1:1	526	1.29×10^{-8}	–32.5
AuNP**3**	1.2:1	526	9.47×10^{-8}	–35.6
AuNP**4**	1.2:1	526	9.47×10^{-8}	
AuNP**5**	1.2:1	524	1.18×10^{-8}	–37.3
AuNP**6**	1.2:1	520	5.79×10^{-9}	–35.9
AuNP**7**	4:1	525	8.32×10^{-9}	–36.2
AuNP**8**	1.5:1	524	1.13×10^{-8}	–24.0[c]

[a] Dispersed in buffered aqueous solution (MOPS, pH 7). [b] ZP = –37.5 mV for TA-capped AuNPs. [c] Suspended in deionized water.

AuNP**1** experienced aggregation during the functionalization reaction and this prevented its use in the detection studies. The other gold nanoparticles remained stable in cold, buffered aqueous solution for at least a month, which is in agreement with their high zeta-potential values in this medium.

Figure 3 (a) shows the Au 4f core level spectra measured by XPS for the samples AuNP**2**, AuNP**5** and AuNP**7** as well as for TA- and citrate-capped AuNPs. The presence of Au was detected in all of them, although the Au 4f doublets measured in the functionalized samples tend to shift to higher binding energies with respect to the unfunctionalized sample. This fact can be attributed to charge-transfer effects between the Au nanoparticles and the incorporated ligands, indicating that Au tends to donate electrons.

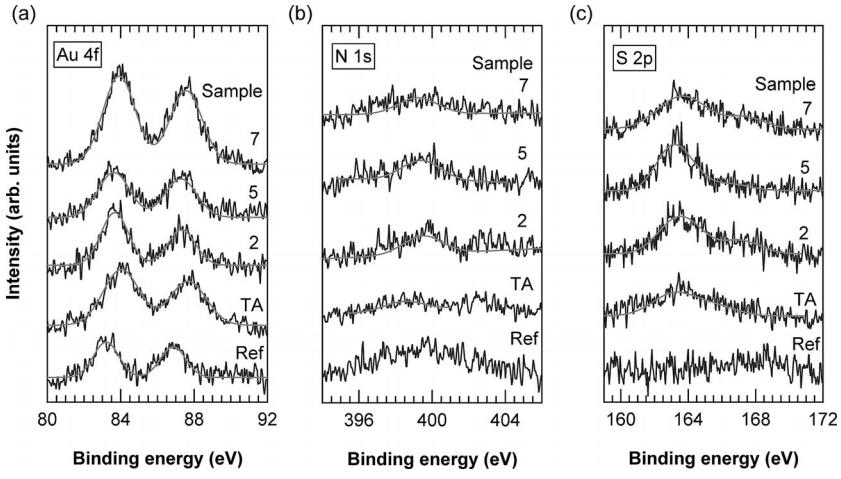

Figure 3. XPS spectra for Au, N and S atoms in AuNP**2**, AuNP**5**, AuNP**7**, TA-capped and citrate-capped (reference) AuNPs.

Figure 3 (b,c) show the N 1s and S 2p core level spectra measured by XPS, respectively. In most of the samples a weak but distinguishable feature attributable to a signal of the N 1s core level can be observed at binding energies of around 400 eV, but is not detectable in the TA-functionalized AuNP nor in the reference sample. In the binding energy region corresponding to the S 2p core level, a clear structure emerges between 160 and 172 eV in the functionalized samples. In these samples, the S 2p spectra appear to be dominated by photoelectrons with binding energies of around 162–163 eV, which can be attributed to sulfur atoms bound and unbound to the gold surface, accompanied by a weaker structure appearing at around 168 eV attributable to oxidized S atoms.

Sensing Studies

To verify the reactivity of the pyridine ligands with the DCNP simulant, a preliminary study was conducted with free ligands **5**–**7** in acetonitrile (the lack of absorption of ligands **1**–**4** in the UV/Vis region precluded their study).

The UV/Vis spectra of ligands **5** and **6** in acetonitrile (5×10^{-5} M) show a band centred at 316 and 431 nm ($\log\varepsilon$ = 4.36 and 4.31 $M^{-1}cm^{-1}$), respectively. The addition of 30 equiv. of DCNP to each ligand induced in both cases a bathochromic shift to give a new band centred at 340 and 532 nm, respectively, corresponding to the phosphorylation of the pyridine moiety, which enhances the intramolecular charge-transfer process in the dyes. The UV spectrum of ligand **7** in acetonitrile (5×10^{-5} M) shows a band centred at 454 nm ($\log\varepsilon$ = 4.15 $M^{-1}cm^{-1}$). In this case, addition of 30 equiv. of DCNP induced the appearance of two broad absorption bands, which, upon deconvolution, split into four well-defined bands at 394, 431, 507 and 537 nm (see Figure 4). Based on previous studies,[6] these bands were assigned to ligand **7** protonated at the dimethylamino group (band centred at 431 nm, confirmed by the addition of 30 equiv. of HCl to a sample of ligand **7** in acetonitrile) and ligand **7** phosphorylated in three different places. The band centred at 537 nm, which corresponds to the phosphorylation of the pyridine moiety, increases the pull–push character of the chromophore, which accounts for the bathochromic shift similar to ligand **6**. The bands at 394 and 507 nm can be assigned to the phosphorylation of the dimethylamino and azo groups of the ligand. The phosphorylation of the aniline moiety was expected to induce a decrease in the charge-transfer character of dye **7**, as we previously observed for a similar system.[6]

On the basis of these results we expected that the phosphorylation of the pyridine moiety in nanoparticles AuNP**2**–AuNP**7** or the formation of an ammonium salt in AuNP**8** promoted by the presence of DCNP would change the overall electrostatic charge on the surfaces of the nanoparticles, triggering an aggregation process coupled with a bathochromic shift of the SPR absorption band and a change in the color of the solution.

In fact, when DCNP (5×10^{-2} M, in acetonitrile) was added to a suspension of the prepared AuNP**2**–AuNP**8** in aqueous MOPS solutions, a color change from red wine to purple blue was readily observed by the naked eye. This change is indicative of the aggregation of AuNPs. The sensing experiments were carried out in buffered solutions to prevent any acidic system slowing or even interfering in the sensing process. DFP and DCP could not be studied because they were hydrolysed in this medium.

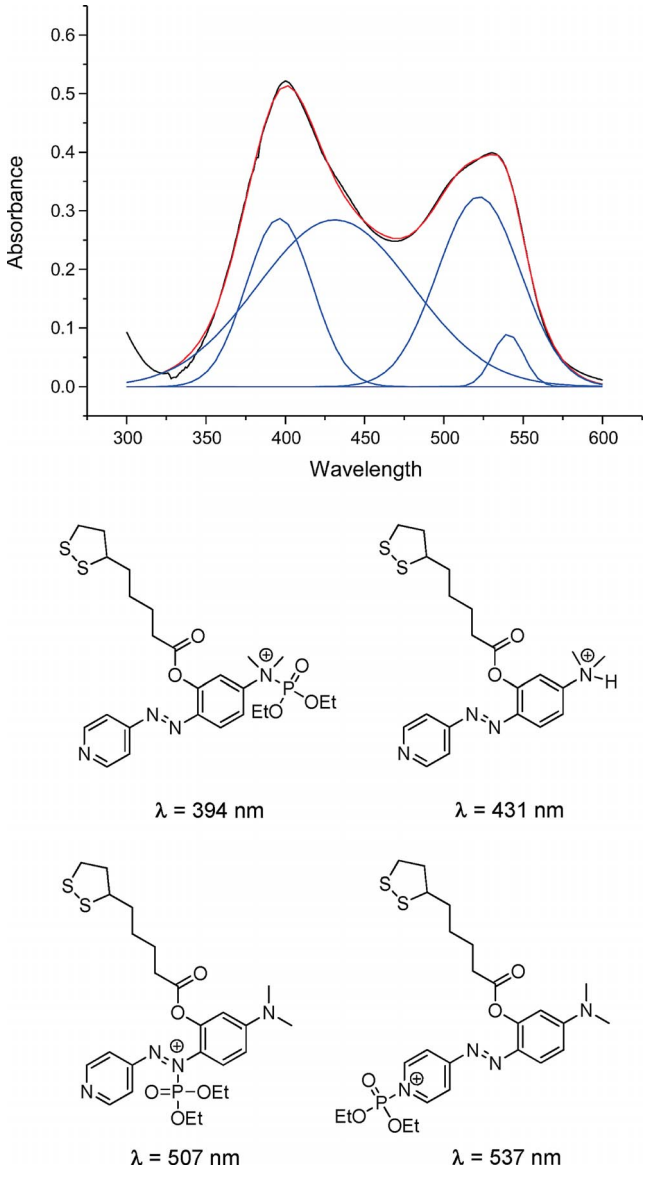

Figure 4. UV/Vis spectrum of ligand **7** (5×10^{-5} M in acetonitrile) on addition of 30 equiv. of DCNP. Deconvolution of the two bands and assigned products.

The ability of these functionalized AuNPs to act as probes for DCNP detection was studied by UV/Vis spectroscopy. The UV/Vis spectra are consistent with the observed color changes. Thus, the intensity of the surface plasmon peak of the monodispersed AuNPs at 526 nm (A_{526}) decreased and a new peak at around 660 nm (A_{660}) appeared as clusters of AuNP formed. Figure 5 shows the results of UV/Vis titration studies performed with AuNP**3** and AuNP**6**, as representative examples, in the presence of

increasing amounts of DCNP. Such changes in the spectra, concomitant with the change in color of the solution, can be well explained by the DCNP-induced aggregation of the nanoparticles through charge neutralization at the surface. The aggregation of the AuNPs was further confirmed by TEM analysis (see Figure 6 for AuNP**3**).

The variation in A_{670}/A_{526} versus DCNP concentration for AuNP**3** and AuNP**6** is also presented in Figure 5. A very significant increase in the A_{660}/A_{526} ratio was observed as the concentration of DCNP was increased, above 600 ppm for AuNP**3** and above 200 ppm for AuNP**6**, which reflects the greater nucleophilic character of ligand **6**. The

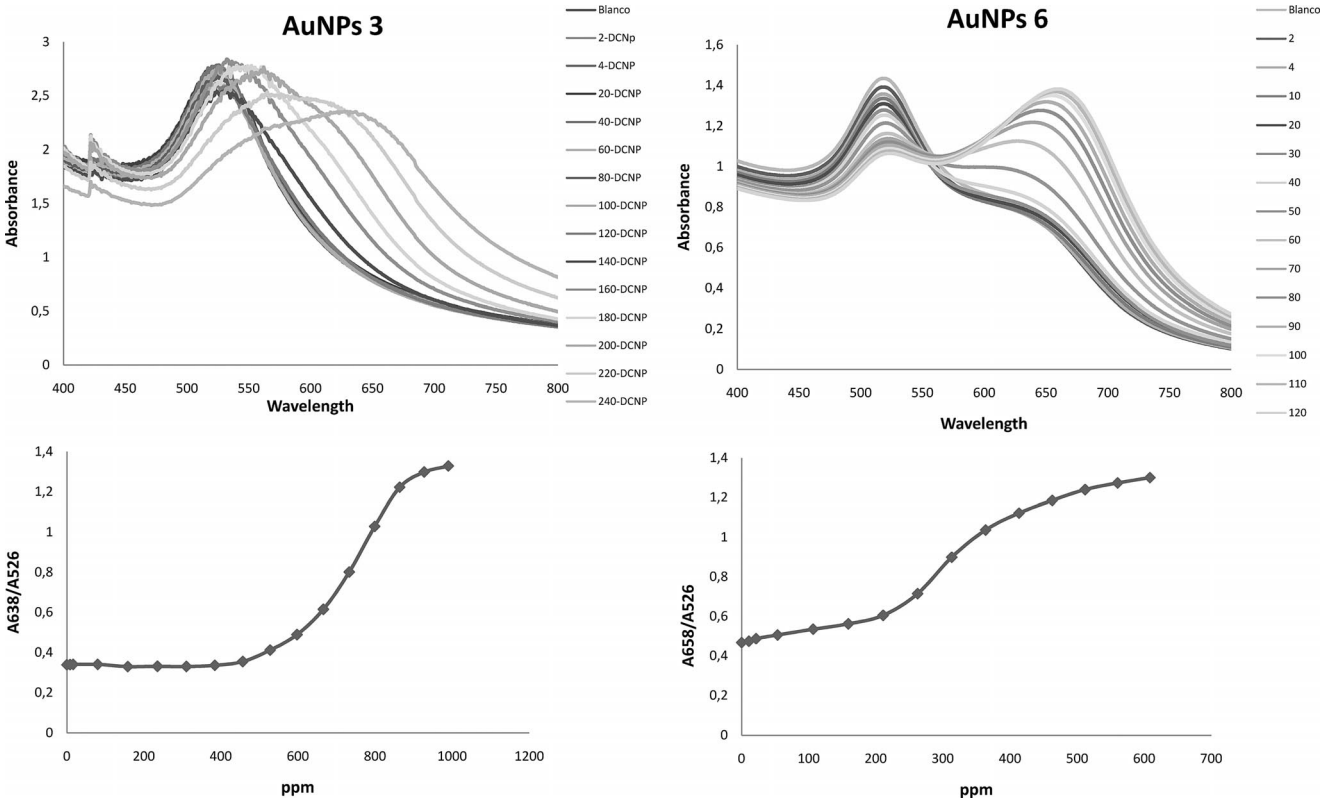

Figure 5. UV/Vis spectra of AuNP**3** (top left) and AuNP**6** (top right) on addition of increasing amounts of DCNP (5×10^{-2} M in acetonitrile) expressed in ppm (mg/L). Plots of A_{660}/A_{526} vs. DCNP concentration for AuNP**3** (bottom left) and AuNP**6** (bottom right).

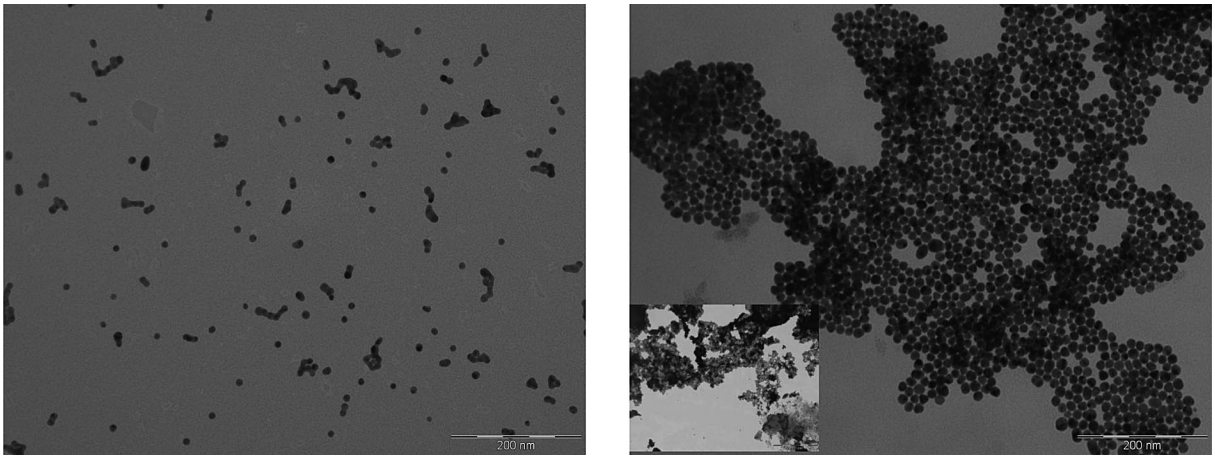

Figure 6. TEM images of a stabilized AuNP**3** dispersion (left) and its aggregates (right) upon addition of excess DCNP at a resolution of 200 nm (inset: the same aggregates at a resolution of 1000 nm).

visual limits of detection (visual LODs, defined as the minimum concentration of simulant necessary for an observable colour change) and calculated LODs (from the changes in UV/Vis spectra, see the Supporting Information) observed for DCNP are presented in Table 2.

Table 2. Visual and calculated LODs of DCNP with AuNP**1**–AuNP**8**.

	AuNP**2**	AuNP**3**	AuNP**4**	AuNP**5**	AuNP**6**	AuNP**7**	AuNP**8**
Visual LOD [ppm]	456	597	1151	310	158	796	106
Calcd. LOD [ppm]	229	470	>1100	340	76	750	81

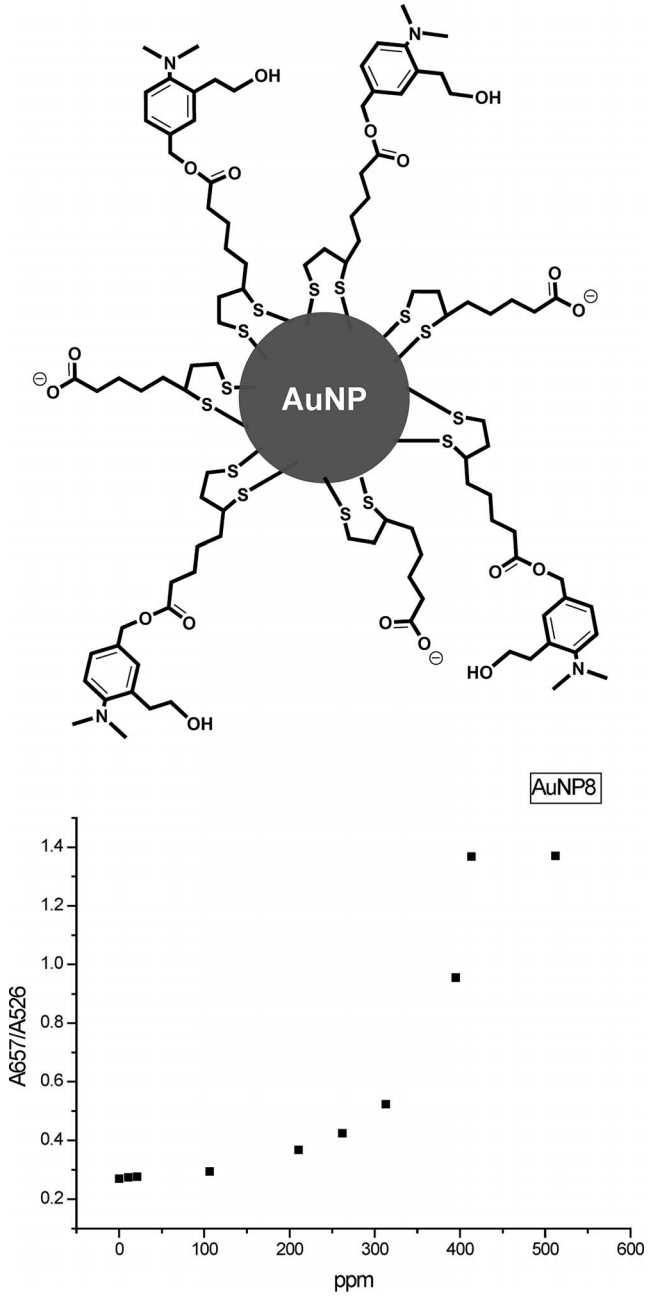

Figure 7. Representation of a AuNP functionalized with ligand **8** (top). Plot of A_{660}/A_{526} vs. DCNP concentration (left).

As expected, AuNP**4** and AuNP**7** showed modest results, probably due to strong steric hindance of the aliphatic ester chain near the pyridine nucleophile, which prevents access of the organophosphate agent to the nitrogen centre. The greater nucleophilic character of the azo-substituted pyridines in ligands **5** and **6** in comparison with ligand **3** would explain the higher LOD observed for the latter.

The best results were obtained with the gold nanoparticles functionalized with azo dye **6** (AuNP**6**) and the dimethylaminophenylethanol ligand **8** (AuNP**8**; Figure 7), which can detect 76 and 81 ppm of DCNP, respectively, thus improving the limit previously obtained by us in solution by a similar approach (see Scheme 1, b).[6]

To demonstrate the selectivity of the system, studies were undertaken that confirmed that AuNP**3**, AuNP**4**, AuNP**5** and AuNP**8** showed only modest responses in their UV/Vis spectra with some of the interference agents that may be present in military or civilian settings such as some pesticides (malathion, dyfonate, 4,4′-DDD, 4,4′-DDE) and gasoline and diesel fuel at concentrations of 2.4 mM in buffered aqueous solution (see Figure S15 in the Supporting Information). No changes in the color of the solutions could be observed with any of these interferents, the gold nanoparticles remaining stable as a red monodispersion.

Conclusions

Functionalized AuNPs have proven to be an interesting alternative for the direct colorimetric detection of nerve agents in buffered aqueous media provided suitable ligands are anchored to the surfaces of the AuNPs. We have achieved detection limits of 76 and 81 ppm (mg/L) for ligands **6** and **8** and found that both steric and electronic effects are crucial for obtaining good results.

Experimental Section

General Procedures: All reagents were commercially available and used without purification. Silica gel 60 F_{254} (Merck) plates were used for TLC. Milli-Q ultrapure water was used for the synthesis of the AuNPs and in the sensing experiments. ^{1}H and ^{13}C NMR spectra were recorded with a Bruker 300 MHz spectrometer. Chemical shifts are reported in ppm with tetramethylsilane as an internal standard. High-resolution mass spectra were recorded in the positive ion mode with a VG-AutoSpec mass spectrometer. UV/Vis absorption spectra were recorded in a 1 cm pathlength quartz cuvette with a Shimadzu UV-2101PC spectrophotometer. All measurements were carried out at 293 K (thermostatted). Zeta potentials were measured with a Malvern Zetasizer ZS three times in 10–25 cycles. X-ray photoelectron spectroscopy (XPS) was employed to verify the success of the molecular modification of the AuNP surfaces. The spectra were recorded with an Escalab 210 spectrometer from Thermo VG Scientific. The base pressure in the analysis chamber was 1.0×10^{-10} mbar. Photoelectrons were extracted by using the Mg-K_α excitation line ($h\nu$ = 1253.6 eV). The binding energy of the spectra refers to the Fermi level. The electronic images

were obtained with a JEOL-1010 transmission electron microscope operating at 100 kV.

Ligands **1** and **2** were commercially available and were used as received.

Synthesis of Ligand 3: Dicyclohexylcarbodiimide (DCC; 5.19 g, 25.2 mmol) was added portionwise to a cold solution of pyridine-4-methanol (2.72 g, 13.2 mmol) in dichloromethane (DCM; 20 mL). Then thioctic acid (2.72 g, 13.2 mmol) and 4-(dimethylamino)pyridine (DMAP; catalytic amounts) in DCM (20 mL) were added and the mixture was stirred for 72 h at room temperature. Then aq. NH_4Cl was added and the resulting precipitate was removed and the remaining solution was extracted with DCM (3× 10 mL). The combined organic layers were washed with water and then dried with $MgSO_4$. The solvent was evaporated and the crude product was purified by column chromatography (silica gel, DCM/AcOEt, 1:1) to yield the corresponding ester **3** (2.04 g, 52%) as a yellow oil. ^{1}H NMR (300 MHz, CD_3OD): δ = 8.52 (dd, J = 4.5, 1.7 Hz, 2 H), 7.45–7.38 (m, 2 H), 5.19 (s, 2 H) 3.56 (ddd, J = 12.2, 8.6, 6.3 Hz, 1 H), 3.22–3.03 (m, 2 H), 2.51–2.38 (m, 3 H), 1.94–1.80 (m, 1 H), 1.76–1.59 (m, 4 H), 1.55–1.41 (m,2 H) ppm. ^{13}C NMR (75 MHz, CD_3OD): δ = 175.0, 150.7, 124.0, 65.5, 58.0, 41.7, 39.8, 36.1, 35.1, 30.2, 26.2 ppm. HRMS: calcd. for $C_{14}H_{19}NO_2S_2$ $[M]^+$ 297.0857; found 297.0832.

Synthesis of Ligand 4: Thioctic acid (2.00 g, 9.69 mmol), Ph_3P (3.05 g, 11.6 mmol) and 2,2′-dipyridyl disulfide (2.56 g, 11.6 mmol) were dissolved in THF (30 mL). The solution was stirred at room temperature for 24 h under argon and then concentrated in vacuo to give the crude product. Purification by column chromatography (hexane/EtOAc, 2:1) afforded 2.26 g (78%) of ligand **4**[21] as a yellow oil. ^{1}H NMR (400 MHz, $CDCl_3$): δ = 8.58 (ddd, J = 4.8, 2.0, 0.8 Hz, 1 H), 7.59 (d, J = 7.6 Hz, 1 H), 7.71 (dt, J = 8.0, 2.0 Hz, 1 H), 7.26 (ddd, J = 7.6, 5.2, 1.2 Hz, 1 H), 3.53 (q, J = 6.4 Hz, 1 H), 3.17–3.04 (m, 2 H), 2.69 (t, J = 7.4 Hz, 2 H), 2.42 (sext, J = 6.8 Hz, 1 H), 1.87 (sext, J = 6.8 Hz, 1 H), 1.77–1.63 (m, 4 H), 1.43–1.53 (m, 2 H) ppm. ^{13}C NMR (75 MHz, $CDCl_3$): δ = 196.0, 151.2, 150.1, 137.2, 130.1, 123.5, 56.1, 43.8, 40.1, 38.4, 34.5, 28.4, 25.0 ppm.

Synthesis of Ligand 5: Phenol (5.0 g, 53 mmol) and sodium nitrite (4.0 g, 58 mmol) in aqueous NaOH (10% w/w, 20 mL) was added dropwise to a solution of 4-aminopyridine (6.0 g, 64 mmol) in 7.3 M HCl (45 mL) at 0 °C. The pH of the mixed solution was adjusted to pH 6–7 by the addition of a 10% aqueous solution of NaOH. The resulting mixture was stirred at 0 °C for 2 h. After neutralization of the solution with sodium hydrogen carbonate, an orange precipitate was obtained. Purification by crystallization with methanol and DCM afforded 4-(4-hydroxyphenylazo)pyridine[22] (4.6 g, 44%) as an orange solid. ^{1}H NMR (300 MHz, $CDCl_3$): δ = 10.57 (s, 1 H), 8.77 (d, J = 6.0 Hz, 2 H), 7.90–7.85 (m, 2 H), 7.68 (dd, J = 4.5, 1.6 Hz, 2 H), 7.02–6.94 (m, 2 H) ppm.

DCC (0.988 g, 4.79 mmol) was added portionwise to a cold solution of 4-(4-hydroxyphenylazo)pyridine (0.454 g, 2.28 mmol) in DCM (20 mL),. Then a cold solution of thioctic acid (0.518 g, 2.51 mmol) and a catalytic amount of DMAP in DCM (20 mL) was added and the mixture was stirred for 72 h at room temperature. After this time, a saturated aqueous solution of ammonium chloride was added and the resulting precipitate was removed. The mixture was extracted with DCM (3× 10 mL). The combined organic layers were washed with water, dried with $MgSO_4$, evaporated and further purified by column chromatography (DCM/AcOEt, 1:1) to yield the corresponding ester **5** (0, 353 g, 40%) as an orange solid. ^{1}H NMR (300 MHz, CD_3OD): δ = 8.77 (d, J = 6.4 Hz, 2 H), 8.06 (d, J = 9.1 Hz, 2 H), 7.84 (d, J = 6.4 Hz, 2 H), 7.36 (d, J = 9.1 Hz, 2 H), 3.68–3.54 (m, 1 H), 3.22–3.06 (m, 2 H), 2.67 (t, J = 7.3 Hz, 2 H), 2.57–2.43 (m, 1 H), 1.95–1.86 (m, 1 H), 1.84–1.69 (m, 4 H), 1.65–1.55 (m, 2 H) ppm. ^{13}C NMR (75 MHz, CD_3OD): δ = 172.37, 153.42, 144.38, 134.38, 134, 06, 129.61, 127.14, 123.05, 121.49, 56.81, 40.23, 38.56, 34.66, 33.57, 28.01, 24.64 ppm. HRMS: calcd. for $C_{19}H_{22}N_3O_2S_2$ $[MH]^+$ 388.1153; found 388.1157.

Synthesis of Ligand 6: 4-aminopyridine (0.367 g, 4 mmol) was dissolved in a mixture of concentrated phosphoric acid (25 mL) and concentrated nitric acid (12 mL). This solution was slowly added to a solution containing sodium nitrite (0.334 mg, 4.8 mmol) and water (8 mL) at –5 °C. The generated diazonium salt was immediately added to a solution containing 2-[methyl(phenyl)amino]ethanol (0.609 mg, 4.03 mmol) and 30% phosphoric acid (20 mL). The reaction mixture was allowed to react for 30 min at –5 °C and then for 60 min at room temperature. The final dark-red crude was neutralized with a saturated sodium carbonate solution and the organic product extracted with DCM. The organic layer was dried with $MgSO_4$, filtered and the solvent eliminated in a rotary evaporator. 4-Azidopyridine (0.234 g, 0.53 mmol, 45%) was isolated as a dark-red solid by column chromatography using AcOET/hexane (1:1) as eluent. ^{1}H NMR (300 MHz, $CDCl_3$): δ = 8.71 (dd, J = 4.6, 1.6 Hz, 2 H), 7.90 (d, J = 9.3 Hz, 2 H), 7.63 (dd, J = 4.6, 1.6 Hz, 2 H), 6.82 (d, J = 9.3 Hz, 2 H), 3.89 (m, 2 H), 3.66 (t, 2 H), 3.16 (s, 3 H) ppm. ^{13}C NMR (75 MHz, $CDCl_3$): δ = 149.72, 159.68, 148.34, 130.95, 120.83, 113.14, 11.52, 63.92, 58.47, 41.04 ppm. HRMS: calcd. for $C_{14}H_{16}N_4O$ $[M]^+$ 256.303; found 256.286.

DCC (1.04 mmol) was added portionwise to a cold solution of (*E*)-2-{methyl[4-(pyridin-4-yldiazenyl)phenyl]amino}ethanol (0.87 mmol) in DCM (25 mL). Then a cold solution of thioctic acid (1.04 mmol) and DMAP (catalytic amount) in DCM (25 mL) was added and the mixture was stirred for 48 h at room temperature. After this time a saturated solution of ammonium chloride was added and the precipitated removed. The mixture was extracted with DCM (3× 10 mL) and the combined organic layers were washed with water, dried with $MgSO_4$, evaporated and further purified by column chromatography (DCM/ethyl acetate, 1:1) to yield the corresponding ester **6** (0.243 g, 45%) as a dark-orange solid. ^{1}H NMR (300 MHz, MeOD): δ = 8.70 (d, J = 6.2 Hz, 2 H), 7.96–7.85 (m, 2 H), 7.72–7.64 (m, 2 H), 6.84–6.73 (m, 2 H), 4.31 (t, J = 5.8 Hz, 2 H), 3.73 (t, J = 5.8 Hz, 2 H), 3.56–3.42 (m, 1 H), 3.14–3.09 (m, 2 H), 3.14–3.09 (s, 3 H), 2.48–2.33 (m, 1 H), 2.24 (t, J = 7.3 Hz, 2 H), 1.92–1.76 (m, 1 H), 1.69–1.51 (m, 4 H), 1.47–1.32 (m, 2 H) ppm. ^{13}C NMR (75 MHz, $CDCl_3$): δ = 173.70, 158.93, 150.09, 126.74, 116.82, 112.04, 60.81, 56.70, 51.22, 40.62, 39.29, 38.87, 34.95, 29.97, 24.88 ppm. ^{13}C NMR (75 MHz, $CDCl_3$): δ = 173.7, 159.2, 153.0, 144.4, 126.8, 116.9, 112.0, 61.6, 56.7, 51.2, 40.6, 38.9, 35.0, 34.3, 29.1, 24.9 ppm. HRMS: calcd. for $C_{22}H_{28}N_4O_2S_2$ $[M]^+$ 444.165; found 444.169.

Synthesis of Ligand 7: 4-Aminopyridine (0.121 g, 1.29 mmol) was dissolved in water (10 mL). Then concentrated sulfuric acid (0.5 mL, 9.2 mmol) was added and the reaction mixture was heated to give a solution. The reaction mixture was cooled to 0 °C and then a solution of $NaNO_2$ (0.089 g, 1.29 mmol) in water (5 mL) was added dropwise. Then a solution of (dimethylamino)phenol (0.206 g, 1.5 mmol) was added dropwise during 30 min. The resulting orange solution was stirred for 30 min at 0 °C and then for 30 min at room temperature. Then the reaction mixture was neutralized with an aqueous saturated solution of potassium acetate (30 mL). The precipitate was purified by column chromatography (hexane/ethyl acetate, 9:1) to yield (*E*)-5-(dimethylamino)-2-(pyridin-4-yldiazenyl)phenol (0.122 g, 39%) as a brown solid. ^{1}H NMR (300 MHz, $CDCl_3$): δ = 15.62 (s, OH), 8.59 (s, 1 H), 7.45 (d,

J = 6.1 Hz, 2 H), 7.32 (d, J = 9.3 Hz, 1 H), 6.52 (dd, J = 9.2, 2.6 Hz, 1 H), 5.91 (d, J = 2.6 Hz, 1 H), 5.30 (s, 1 H), 3.17 (s, 6 H) ppm. ^{13}C NMR (75 MHz, $CDCl_3$): δ = 159.72, 158.91, 151.87, 148.37, 131.14, 114.01, 104.12, 99.18, 96.25, 41.29 ppm. HRMS: calcd. for $C_{13}H_{14}N_4O$ $[M]^+$ 242.1168; found 242.1194.

DCC (1.392 mmol) was added portionwise to a cold solution of (*E*)-5-(dimethylamino)-2-(pyridin-4-yldiazenyl)phenol (0.87 mmol) in DCM (25 mL). Then a cold solution of thioctic acid (1.04 mmol) and DMAP (catalytic amount) in DCM (25 mL) was added and the mixture was stirred for 48 h at room temperature. After this time, a saturated solution of ammonium chloride was added and the precipitate removed. The mixture was extracted with DCM (3× 10 mL) and the combined organic layers were washed with water, dried with $MgSO_4$, evaporated and further purified by column chromatography (DCM/ethyl acetate, 1:1) to yield the corresponding ester **7** (0.150 g, 40%) as an orange solid. ^{1}H NMR (300 MHz, $CDCl_3$): δ = 8.64 (dd, J = 4.6, 1.6 Hz, 1 H), 7.79 (d, J = 9.3 Hz, 1 H), 7.49 (dd, J = 4.6, 1.6 Hz, 2 H), 6.54 (dd, J = 9.3, 2.8 Hz, 1 H), 6.36 (d, J = 2.7 Hz, 1 H), 3.50 (dq, J = 13.2, 6.6 Hz, 1 H), 3.07 (s, 2 H), 3.08–3.04 (m, 3 H), 2.62 (t, J = 7.4 Hz, 1 H), 2.40 (dq, J = 6.6, 5.5 Hz, 1 H), 2.30 (t, J = 7.3 Hz, 2 H), 1.93–1.78 (m, 3 H) ppm. ^{13}C NMR (75 MHz, $CDCl_3$): δ = 172.4, 159.7, 151.7, 148.2, 142.0, 130.1, 113.0, 108.3, 104.7, 96.4, 56.4, 41.2, 40.3, 38.7, 34.6, 33.5, 28.1, 24.6 ppm. HRMS: calcd. for $C_{21}H_{26}N_4O_2S_2$ $[M]^+$ 430.150; found 430.146.

Synthesis of Ligand 8: 2-(2-Nitrophenyl)ethanol (2.3 g, 19.67 mmol), formaldehyde (4.83 mL, 32.3 mmol, 36%) and Pd/C (480 mg, 10%) were dissolved in absolute ethanol (200 mL) and placed under H_2 until uptake of hydrogen had ceased. After filtration through Celite, the solvent was evaporated and the product was purified by extraction with ethyl acetate and washed with water. The organic layer was washed with brine and dried with $MgSO_4$ to give 2-(dimethylaminophenyl)ethanol (**10**; 3.22 g, 95%) as a yellow oil. ^{1}H NMR (300 MHz, $CDCl_3$): δ = 7.19–6.95 (m, 4 H), 3.76 (t, J = 5.9 Hz, 2 H), 2.91 (t, J = 5.7 Hz, 2 H), 2.62 (s, 6 H) ppm. ^{13}C NMR (75 MHz, $CDCl_3$): δ = 152.6, 136.5, 131.5, 128.0, 125.4, 120.4, 64.7, 45.4, 36.5 ppm.

NBS (0.187 g, 1.05 mmol) was added to a mixture of 2-(dimethylaminophenyl)ethanol (**10**; 0.165 g, 1 mmol) and NH_4OAc (10 mol-%) in MeCN (5 mL) and the mixture was stirred at room temperature. After completion of the reaction as indicated by TLC, the mixture was concentrated in vacuo and extracted with EtOAc/H_2O (1:1, 3× 5 mL). The organic portion was separated from the extract, dried and concentrated. The residue was subjected to column chromatography (silica gel, hexane/EtOAc, 10:1) to obtain pure 2-(5-bromo-2-dimethylaminophenyl)ethanol (**11**) as a brown oil. (0.237, 97%). ^{1}H NMR (300 MHz, $CDCl_3$): δ = 7.23 (dt, J = 8.4, 2.4 Hz, 2 H), 6.95 (t, J = 7.1 Hz, 2 H), 4.86 (s, 1 H), 3.73 (t, J = 6.2 Hz, 2 H), 2.92–2.8 (m, 2 H), 2.57 (s, 6 H) ppm. ^{13}C NMR (75 MHz, $CDCl_3$): δ = 151.8, 138.9, 134.2, 130.9, 122.3, 118.2, 64.5, 45.4, 36.2 ppm.

2-(5-Bromo-2-dimethylaminophenyl)ethanol (**11**; 1.75 g, 7.14 mmol) and imidazole (1.46 g, 21.44 mmol) was dissolved in anhydrous DCM (5 mL). *tert*-Butyldimethylsilyl chloride (1.19 g, 7.86 mmol) was added and the reaction mixture was stirred at room temperature until the complete disappearance of the starting material (by TLC). The solvent was evaporated and the residue dissolved in ethyl acetate (20 mL) and washed with concentrated aqueous $NaHCO_3$ (2× 10 mL). The organic layer was dried with $MgSO_4$ and the solvents evaporated. The product was purified by column chromatography (DCM/MeOH, 95:5) to give 4-bromo-2-{2-[(*tert*-butyldimethylsilyl)oxy]ethyl}-*N*,*N*-dimethylaniline (**12**; 0.2106 g, 83%) as a pale-yellow oil. ^{1}H NMR (300 MHz, $CDCl_3$): δ = 7.37–7.18 (m, 2 H), 6.94 (d, J = 8.5 Hz, 1 H), 3.81 (t, J = 7.25 Hz, 2 H), 2.87 (t, J = 7.0 Hz, 2 H), 2.62 (s, 6 H), 0.86 (s, 9 H), 0.00 (s, 6 H) ppm. ^{13}C NMR (75 MHz, $CDCl_3$): δ = 152, 137.03 133.18, 131.2, 121.82, 118.1, 63.82, 45.60, 34.64, 26.33, 18.74, –5.01 ppm. HRMS: calcd. for $C_{16}H_{28}BrNOSi$ $[M]^+$ 357.1124; found 357.1192.

A solution of bromide **12** (1.49 g, 4.15 mmol) dissolved in THF (30 mL) was cooled to –78 °C under Ar. *n*-Butyllithium (6.5 mL, 5 mmol) was added dropwise with stirring and then warmed to 0 °C and kept at this temperature for an additional 1 h. Again the solution was cooled to –78 °C and dry dimethylformamide (0.96 mL, 12.48 mmol) was added. The reaction was stirred at room temperature for 2 h and water (15 mL) was added. The solvents were removed in vacuo and the residue redissolved in DCM. The organic extract was dried with anhydrous $MgSO_4$ and filtered. 3-{2-[(*tert*-Butyldimethylsilyl)oxy]ethyl}-4-dimethylaminobenzaldehyde (**13**) was obtained after silica gel column chromatography (ethyl acetate/hexane, 1:5) in 98% yield (1.26 g). ^{1}H NMR (300 MHz, $CDCl_3$): δ = 9.83 (s, 1 H), 7.76 (d, J = 2.1 Hz, 1 H), 7.68 (dd, J = 8.3 and 2.1 Hz, 1 H), 7.07 (d, J = 8.3 Hz, 1 H), 3.86 (t, J = 7.0 Hz, 2 H), 2.93 (t, J = 7.0 Hz, 2 H), 2.78 (s, 6 H), 0.84 (s, 9 H), –0.02 (s, 6 H) ppm. ^{13}C NMR (75 MHz, $CDCl_3$): δ = 191.8, 159.2, 133.2, 132.8, 130.9, 129.7, 118.9, 67.9, 63.5, 50.3, 45.8, 44.7, 35.2, 31.4, 26.4, 26.3, 18.7, –5.0 ppm. HRMS: calcd. for $C_{17}H_{29}NO_2Si$ $[M]^+$ 307.1968; found 307.2036.

$NaBH_4$ (0.034 g, 9.0 mmol) was added to a solution of **13** (0.461 g, 15 mmol) in MeOH (30 mL), and the mixture was heated at 60 °C for 2.5 h. After addition of water (20 mL) at 0 °C, work-up was performed with ethyl acetate and water, and the combined organic layers were washed with brine and dried with $MgSO_4$. After filtration followed by evaporation, the residue was subjected to column chromatography through silica gel (ethyl acetate/hexane, 3:7) to afford pure 3-{2-[(*tert*-butyldimethylsilyl)oxy]ethyl}-4-[(dimethylamino)phenyl]methanol (**14**; 0.424 g, 91%) as a pale-yellow solid. ^{1}H NMR (300 MHz, $CDCl_3$): δ = 7.23–7.13 (m, 2 H), 7.13–7.05 (m, 1 H), 4.59 (s, 2 H), 3.82 (t, J = 7.3 Hz, 2 H), 2.92 (t, J = 7.3 Hz, 2 H), 2.64 (s, 6 H), 1.61 (s, 2 H), 1.35–1.28 (m, 1 H), 0.87 (s, 9 H), 0.01 (s, 6 H) ppm. ^{13}C NMR (75 MHz, $CDCl_3$): δ = 153.3, 136.1, 134.7, 130.1, 126.3, 120.3, 65.7, 64.3, 45.7, 35.1, 26.4, 18.8 ppm. HRMS: calcd. for $C_{19}H_{29}NO_2Si$ $[M]^+$ 309.5190; found 309.1402.

DCC (0.480 g, 2.32 mmol) was added portionwise to a cold of solution of **14** (0.343 g, 1.1 mmol) in DCM (25 mL). Then a solution of thioctic acid (251 mg, 1.65 mmol) and 4-(dimethylamino)pyridine (catalytic amount) in DCM (25 mL) was added and the mixture was stirred for 24 h at room temperature. Then brine was added and the mixture was extracted with diethyl ether (3× 5 mL). The combined organic layers were washed with water, dried with $MgSO_4$, evaporated and further purified by column chromatography (dichloromethane/ethyl acetate, 1:1) to yield **15** (0.243 g, 44%) as a yellow oil. ^{1}H NMR (300 MHz, $CDCl_3$): δ = 7.16 (dd, J = 10.2, 5.0 Hz, 2 H), 7.05 (dd, J = 8.0, 4.4 Hz, 1 H), 5.01 (s, 2 H), 3.81 (t, J = 7.1, 3.5 Hz, 2 H), 3.53 (dt, J = 13.0, 6.5 Hz, 1 H), 3.20–3.03 (m, 2 H), 2.90 (t, J = 7.3, 3.9 Hz, 2 H), 2.65 (s, 5 H), 2.48–2.38 (m, 1 H), 2.33 (t, J = 19.7, 7.0 Hz, 1 H), (dt, J = 19.7, 7.0 Hz, 1 H), 1.71–1.61 (m, 4 H), 1.46 (dt, J = 15.6, 6.8 Hz, 2 H), 0.87 (s, 9 H), 0.00 (s, 6 H) ppm. ^{13}C NMR (75 MHz, $CDCl_3$): δ = 173.8, 153.9, 134.6, 131.4, 130.9, 127.6, 120.1, 66.6, 64.2, 56.7, 45.6, 40.6, 38.9, 35.1, 35.0, 34.5, 29.1, 26.4, 25.1, 18.8, –4.94 ppm. HRMS: calcd. for $C_{25}H_{43}NO_3S_2Si$ $[M]^+$ 497.893; found 497.8244.

TBAF·3H_2O (0.73 mL, 0.7 mmol) was added to a solution of **15** (0.243 mg, 0.5 mmol) in THF (4 mL) and the mixture was stirred

at room temperature for 2 h. The reaction mixture was then diluted with water (10 mL) and the aqueous phase extracted with diethyl ether (5 × 5 mL). The combined organic layers were dried with $MgSO_4$, filtered and the solvent was removed in vacuo. The crude product was purified by column chromatography (hexane/ethyl acetate, 1:1) to furnish the ligand 4-(dimethylamino)-3-(2-hydroxyethyl)benzyl 5-(1,2-dithiolan-3-yl)pentanoate (**8**; 0.064 g, 35%) as a colourless liquid. ^{1}H NMR (300 MHz, $CDCl_3$): δ = 7.18 (dd, J = 10.2, 5.0 Hz, 2 H), 7.05 (dd, J = 8.0, 4.4 Hz, 1 H), 5.01 (s, 2 H), 3.84 (t, J = 7.1, 3.5 Hz, 2 H), 3.53 (dt, J = 13.0, 6.5 Hz, 1 H), 3.20–3.03 (m, 2 H), 2.99 (t, J = 7.3, 3.9 Hz, 2 H), 2.65 (s, 5 H), 2.48–2.38 (m, 1 H), 2.33 (t, J = 19.7, 7.0 Hz, 1 H), (dt, J = 19.7, 7.0 Hz, 1 H), 1.71–1.61 (m, 4 H), 1.46 (dt, J = 15.6, 6.8 Hz, 2 H) ppm. ^{13}C NMR (75 MHz, $CDCl_3$): δ = 173.7, 152.7, 136.8, 132.9, 131.7, 128.1, 120.6, 66.2, 64.7, 56.7, 45.4, 40.6, 38.9, 36.6, 35.0, 34.4, 29.1, 25.1 ppm. HRMS: calcd. for $C_{19}H_{29}NO_3S_2$ $[M]^+$ 383.5683; found 383.1694.

Preparation of the Functionalized AuNPs: All glassware was thoroughly cleaned with freshly prepared aqua regia (HCl/HNO_3, 3:1), rinsed thoroughly with deionized water and dried in air. AuNPs with a diameter of around 13 nm were synthesized as reported previously.[16] Briefly, an aqueous 38.8 mM trisodium citrate solution (10 mL) was added to a boiling solution of 1 mM $HAuCl_4$ (100 mL) and the resulting solution boiled for 30 min until a red solution was obtained. This solution was cooled to room temperature and then stored in a refrigerator at 4 °C for use. The AuNPs were modified by ligand-exchange reaction at room temperature as follows: A 0.01 M aqueous NaOH solution (20 μL) was added to the as-prepared citrate-capped AuNPs (10 mL). Then TA (200 μL, 10^{-3} M in ethanol) and the appropriate amount of ligand **2**–**8** (10^{-3} M in ethanol) were added simultaneously and the solution was stirred overnight. To purify the AuNPs, the mixture was centrifuged for 20 min at 14000 rpm and the supernatants were decanted. Then the resulting AuNPs were resuspended in MOPS buffer solution (0.1 M at pH 7). The size and shape of the modified AuNPs were characterized by TEM. The UV/Vis spectra absorbance spectra of the modified AuNPs were recorded.

The limits of detection (LODs) were determined as described in the Supporting Information

Supporting Information (see footnote on the first page of this article): Copies of the ^{1}H NMR and ^{13}C NMR spectra (Figures S1 to S11), UV/Vis spectra ligands **5**–**7** (Figure S12), UV/Vis spectra and A_{660}/A_{526} vs. DCNP concentration plots for AuNP**2**-AuNP**8** and method of determination of LODs.

Acknowledgments

The authors thank the Spanish Government (grant numbers MAT2009-14564-C04-03 and MAT2012-38429-C04-02) and the Generalitat Valenciana (Project PROMETEO/2009/095) for support. A. M. is grateful to the Spanish Government for a fellowship. SCSIE (Universidad de Valencia) is gratefully acknowledged for all the equipment employed.

[1] a) H. H. Hill Jr., S. J. Martin, *Pure Appl. Chem.* **2002**, *74*, 2285–2291; b) M. Wheelis, *Pure Appl. Chem.* **2002**, *74*, 2247–2251.
[2] S. M. Somani *Chemical Warfare Agents*, Academic Press, San Diego, CA, **1992**.
[3] a) J. J. Gooding, *Anal. Chim. Acta* **2006**, *559*, 137–151; b) L. M. Eubanks, T. J. Dickerson, K. D. Janda, *Chem. Soc. Rev.* **2007**, *36*, 458–470.
[4] S. Royo, R. Martinez-Mañez, F. Sancenón, A. M. Costero, M. Parra, S. Gil, *Chem. Commun.* **2007**, 4839–4847.
[5] A. M. Costero, M. Parra, S. Gil, R. Gotor, P. M. E. Mancini, R. Martinez-Mañez, F. Sancenón, R. Royo, *Chem. Asian J.* **2010**, *5*, 1573–1585.
[6] S. Royo, A. M. Costero, M. Parra, S. Gil, R. Martinez-Mañez, F. Sancenón, *Chem. Eur. J.* **2011**, *17*, 6931–6934.
[7] a) R. Elghanian, J. J. Storhoff, R. C. Mucic, R. L. Letsinger, C. A. Mirkin, *Science* **1997**, *227*, 1078–1081; b) L. M. Wang, X. F. Liu, X. F. Hu, S. P. Song, C. H. Fan, *Chem. Commun.* **2006**, 3780–3782; c) D. B. Liu, W. S. Qu, W. W. Chen, W. Zhong, Z. Wang, X. X. Jiang, *Anal. Chem.* **2010**, *82*, 9606–9610; d) K. Saha, S. S. Agasti, C. Kim, X. Li, V. M. Rotello, *Chem. Rev.* **2012**, *112*, 2739–2779; e) V. K. K. Upadhyayula, *Anal. Chim. Acta* **2013**, *715*, 1–18.
[8] W. Haiss, N. T. K. Thanh, J. Aveyard, D. G. Fernig, *Anal. Chem.* **2007**, *79*, 4215–4221.
[9] B. Kong, A. Zhu, Y. Luo, Y. Tian, Y. Yu, G. Shi, *Angew. Chem.* **2011**, *123*, 1877; *Angew. Chem. Int. Ed.* **2011**, *50*, 1837–1840.
[10] D. Liu, Z. Wang, X. Jiang, *Nanoscale* **2011**, *3*, 1421–1433.
[11] a) K. M. Mayer, J. H. Hafner, *Chem. Rev.* **2011**, *111*, 3828–3857; b) E. E. Bedford, J. Spadovecchia, C. M. Pradier, F. X. Gu, *Macromol. Biosci.* **2012**, *12*, 724–739.
[12] J. Sun, L. Guo, Y. Bao, J. Xie, *Biosens. Bioelectron.* **2011**, *28*, 152–157.
[13] H. Li, J. Guo, H. Ping, L. Liu, M. Zhang, F. Guan, C. Sun, Q. Zhang, *Talanta* **2011**, *87*, 93–99.
[14] K. Bondyopadhyay, S. G. Lin, H. Lin, L. Echegoyen, *Chem. Eur. J.* **2000**, *6*, 4385–4392.
[15] M. Kadalbajoo, J. Park, A. Opdahl, H. Suda, C. A. Kitchens, J. C. Garnó, J. D. Batteas, M. J. Tarlov, P. Deshong, *Langmuir* **2007**, *23*, 700–707.
[16] P. Zhao, N. Li, D. Astruc, *Coord. Chem. Rev.* **2013**, *257*, 638–665.
[17] N. R. Jana, L. Gearheart, C. J. Murphy, *Langmuir* **2001**, *17*, 6782–6786.
[18] a) K. C. Grabar, R. G. Freeman, M. B. Hommer, M. J. Natan, *Anal. Chem.* **1995**, *67*, 735–743; b) K. R. Brow, A. P. Fox, M. J. Natan, *J. Am. Chem. Soc.* **1996**, *118*, 1154–1157.
[19] S.-Y. Lin, Y.-T. Tsai, C.-C. Chen, C.-M. Lin, C.-h. Chen, *J. Phys. Chem. B* **2004**, *108*, 2134–2139.
[20] X. Liu, M. Atwater, J. Wang, Q. Huo, *Colloids Surf. B* **2007**, *58*, 3–7.
[21] M. Kadalbajoo, J. Park, A. Opdahl, H. Suda, C. A. Kitchens, J. C. Garno, J. D. Batteas, M. J. Tarlov, P. DeShong, *Langmuir* **2007**, *23*, 700–707.
[22] L. Cui, Y. Zhao, *Chem. Mater.* **2004**, *16*, 2076–2082.

Received: March 6, 2013
Published Online: June 17, 2013

